NACA TN 2829

NATIONAL ADVISORY COMMITTEE FOR AERONAUTICS

TECHNICAL NOTE 2829

EXPERIMENTS ON TRANSONIC FLOW AROUND WEDGES

By George P. Wood

Langley Aeronautical Laboratory
Langley Field, Va.

Washington
November 1952

NATIONAL ADVISORY COMMITTEE FOR AERONAUTICS

TECHNICAL NOTE 2829

EXPERIMENTS ON TRANSONIC FLOW AROUND WEDGES

By George P. Wood

SUMMARY

Several aspects of transonic flow around the forward portions of wedge profiles were studied by means of interferometry. Measurements were made of the two kinds of flow pattern that occur at the leading edge of a wedge at an angle of attack. The growth of the supersonic region at a sharp convex corner formed by two flat surfaces was also observed. The pressure drag coefficient of a wedge of 14.5° semiangle was measured at Mach numbers of 0.768, 0.819, and 0.854 and was shown to be consistent with those of wedges of smaller angle when plotted according to the transonic similarity law. Conditions at the bases of the shock waves that interacted with boundary layers on the wedge were measured. The method of characteristics was used to calculate the flow behind an experimentally determined sonic line, and the calculated flow field was compared with the measured flow field. The accuracy in the location of the sonic line necessary to give correctly the pressure distribution on the surface behind it was determined.

INTRODUCTION

Observations of the change that occurs in the flow pattern near the leading edge of a symmetrical wedge at an angle of attack greater than the semiangle of the wedge as the subsonic free-stream Mach number is increased were reported in reference 1. This reference showed that, at the lower subsonic Mach numbers, an extensive region of separated flow occurs on the upper surface and, at the higher subsonic Mach numbers, the extensive region of separation is replaced by supersonic flow. In the present experiments an interferometer was used in order to obtain quantitative measurements of these flow fields in more detail than was possible by other means.

Another objective was to show the nature of the flow field at a sharp convex corner formed by two flat surfaces when the flow approaching the corner is subsonic. A series of interferograms was therefore taken of the flow around a modified wedge, or hexagon, from which Mach number contours in the flow field were obtained in order to show the growth of the supersonic region at the corner as the subsonic free-stream Mach number was increased.

From the same series of interferograms the flow along the surface of the wedge forepart of the hexagon (a 14.5° semiangle wedge) was measured to obtain Mach number and pressure distributions and pressure drag coefficients. These pressure drag coefficients are expressed in terms of the transonic similarity rule for comparison with similar data from reference 2 for wedges of smaller semiangles.

Data have also been obtained on the boundary conditions at the bases of the shock waves that occurred near the leading edge of the symmetrical wedge at an angle of attack. The conditions at the bases of shock waves that interact with turbulent and laminar boundary layers on the wedge are given and compared with each other and with those on the circular-arc section described in reference 3.

The present data on the flows about the wedge and the hexagon were used to determine how well the supersonic part of a mixed flow field can be calculated by the method of characteristics from an experimentally determined sonic line. The flow fields behind the sonic lines that start at the leading edge of the wedge and at the corner of the hexagon were calculated and were compared with those obtained from interferograms. The accuracy that is necessary in the location of the sonic line in order to give reasonable accuracy in the calculated Mach number distribution on the surface behind the sonic line was also determined.

SYMBOLS

c	total chord of model
C_p	pressure coefficient, $\frac{p - p_o}{q_o}$
C_D	pressure drag coefficient, $\tau \int_0^1 C_p \, d\frac{x}{c}$
M	Mach number
p	static pressure
Δp	pressure difference across shock wave, $p_2 - p_1$
q	dynamic pressure, $\rho V^2/2$
x	coordinate in direction of longitudinal axis of model
α	angle of attack
γ	ratio of specific heats

δ	angle of deviation of flow by shock wave
ϵ	angle of shock wave
ρ	density
τ	thickness ratio of symmetrical wedge
V	velocity

Subscripts:

o	free stream
1	ahead of shock wave
2	behind shock wave

APPARATUS, MODELS, AND METHOD

The wind tunnel that was used for the experiments was operated by the blow-down of dry, compressed air from a storage tank. The air passed through an automatic pressure regulator and a settling chamber and then through a subsonic nozzle to the atmosphere (fig. 1). The top and the bottom of the test section were open to the atmosphere and the sides were closed by straight extensions of two sides of the nozzle and contained windows of optical-quality glass. The height of the test section was 4 inches and the width was 5 inches; the model completely spanned the test section.

One model was a thin symmetrical wedge of which the included angle of the leading edge was 6° (fig. 2(a)). The chord line of the wedge was placed at an angle of attack of approximately 5.5°. The other model was a hexagon that had a total included angle at the leading edge of 29° and a chord of 1.5 inches (fig. 2(b)). The chord line of the hexagon was set at an angle of attack of 0°. In order to reduce boundary-interference effects on the upper surface, each model was placed below the center line of the test section so that the chord line of the model was 3 inches from the upper boundary and 1 inch from the lower boundary.

The range of Mach number was from 0.620 to 0.933 and the range of Reynolds number per inch of model chord was from 4×10^{5} at the lowest Mach number to 7×10^{5} at the highest Mach number.

Observations were made with a Mach-Zehnder interferometer that had 4-inch plates. The light source utilized a high-voltage magnesium spark that had a duration of 3 microseconds and a monochromator to isolate the region of the green lines. The interferograms were analyzed to obtain density contours by the method of superposing flow and no-flow interferograms. The density contours were converted to Mach number contours under the assumption of constant entropy. Static holes were provided in the model and in one of the glass windows in order to obtain reference pressures for making corrections in the analysis of the interferograms. One correction was for any change in the no-flow fringe spacing that might occur during a test. The other was for the effect of the side-wall boundary layers on the optical-path length of the light through the test section. The methods of making these corrections are described in more detail in reference 3. Both of these corrections were made in all the results in the present paper. As a check on the contours and in order to determine the magnitude of random errors, two interferograms were taken at each free-stream Mach number. Each of these interferograms was analyzed independently and then the contours were superposed and compared. The greatest difference in Mach number at any point on two corresponding interferograms was found to be 0.01 or less for most of the interferograms and 0.03 for a few of the interferograms. The random error in Mach number was therefore generally less than 1 percent. The systematic errors were also estimated and were judged to be about 3 percent.

On the interferograms of the flow about a symmetrical wedge that had a strong normal shock wave, the fringes do not extend monotonically through the region just ahead of the shock wave but bend down sharply some small distance ahead of the shock wave. This bending indicates a change in sign of the derivative of density. The average density across the test section which had been falling in the direction of flow apparently begins to rise as the shock wave is approached. This result is probably a spurious effect that is due to the action of the pressure increase across the shock wave on the boundary layer on the side walls. The effect was ignored in analyzing the interferograms and the contours were extrapolated through the affected region to the shock wave.

RESULTS AND DISCUSSION

Flow at Leading Edge

The interferograms of the flow about the leading edge of the symmetrical wedge airfoil are shown in figure 3, together with the contours of constant Mach number. This series of interferograms clearly shows the phenomenon that was reported in reference 1. At the lower free-stream Mach numbers (0.765 and less in the present case) an extensive separated region is shown on the upper surface, and at the higher Mach numbers

(0.812 and above) the extensive region of separation is eliminated and a supersonic region appears that contains an oblique shock wave and that is followed by a nearly normal shock wave. A number of things can be learned about the flow by a study of figure 3. In the first place, the flow in the large separated region at the lower Mach numbers can be deduced. The manner in which the density varies in that region can be obtained from the interferograms in figures 3(a) and 3(b). In the separated region the density increases in the downstream direction at a rate of approximately 0.7 of free-stream density per inch and the density also increases in a vertical direction upward at about one-fourth that rate. Because the velocities in the region are probably small (the temperature is therefore probably close to stagnation temperature), pressure variations probably closely approximate density variations. The flow in the separated region can then be reasoned to be a vortex flow, as shown in figure 4(a). Along the inside of the mixing zone the fluid can flow against a pressure rise because of the shearing stress. Along the wall the flow reverses because of the decreasing pressure in the upstream direction. At equilibrium, the rate of removal of fluid by the action of viscosity is equal to the rate of addition of fluid by the reverse flow along the surface. For the flow in the upper part of the separated region, centrifugal force is balanced by the pressure rise in the vertical direction, and for the flow along the wall no centrifugal force is present.

Figures 3(a) and 3(b) also show that the pressure in the main flow, just outside of and along the separated region, is not constant but increases from a value corresponding to a Mach number of approximately 1 to a value close to free-stream pressure.

Over the range of free-stream Mach number covered by figure 3, the concentric fringe pattern on the lower surface of the wedge shows that the stagnation point is on the lower surface and very close to the leading edge.

For the type of flow pattern in figures 3(c) to 3(e), the experiments do not directly settle the question of the location of the sonic line at the surface, but they do aid in a discussion of the probable location. The Mach number contours indicate strongly that the sonic line starts from the upper surface. (At the leading edge a blurred region appears on the interferograms, because of refraction of the light in the large density gradient there, that precludes following the contours all the way to the surface.) As is well-known, potential flow around a sharp corner must reach supersonic speeds. If there were no boundary layer, no separation, and the leading edge had zero thickness, the sonic line would have to start on the lower surface. Furthermore, under these conditions there would have to be a large region of cavitation on the upper surface since the flow would have to turn nearly 180°, an amount that is far beyond the maximum possible angle of 130°. There are undoubtedly, however, viscous effects that tend to round off the corner, and the conclusion must be reached that the sonic line does not originate on the lower surface. The flow around the leading edge must therefore be that around a curved surface, and the effective curvature must be due to bluntness of the leading edge (the thickness of the leading edge was less than 0.0008 inch), finite thickness of the boundary layer, or a small region of separation, or some combination of these factors. The probable configuration near the leading edge is that shown in figure 4(b) (for which the data were taken from a larger and more detailed version of fig. 3(d) than appears in this paper), which shows a small separated region at the leading edge. This configuration agrees with that deduced by Mr. John Stack and described by him at the Sixth International Congress for Applied Mechanics at Paris in September 1946.

The oblique and the normal shock waves on the wedge and the familiar lambda shock wave that occurs on curved airfoils form the same general kind of shock-wave pattern. It is interesting to note, however, that the oblique shock wave on the wedge is caused by reattachment of the flow whereas the forward leg of the lambda shock wave on a curved surface is caused by separation of the flow.

In the schlieren photographs of reference 1, two shock waves originate at the leading edge. In the present experiments with dry air there is only one shock wave. The extra shock wave in reference 1 was possibly due to condensation of water vapor.

The slip line (or vortex sheet) behind the juncture of the oblique and the "normal" shock waves can be clearly seen in figures 3(c) and 3(d).

Flow Around Corner

The interferograms of the flow about the hexagonal section are shown in figure 5, together with the contours of constant Mach number that are derived from analysis of the interferograms. (Mach number contours are not shown for the two interferograms taken at the higher free-stream Mach numbers because the shock wave probably reached the jet boundary and the quantitative effect of the boundary on the flow field under that condition is not known.) The growth of the supersonic region at the corner can easily be observed in figure 5 (which is similar to fig. 9 of ref. 2). At a free-stream Mach number of 0.620 (fig. 5(a)), no supersonic zone at the corner is apparent. At the next higher speed (fig. 5(b)), there is a small supersonic zone followed by a small, weak shock wave. As the free-stream Mach number is increased further, the supersonic region increases in size and is followed by a shock wave that is nearly normal over most of its length. At the higher Mach numbers the shock wave is not a true lambda shock wave, since the line on the interferograms that begins near the corner and that might be taken to be the forward leg of a lambda shock wave is actually only the end of an expansion region and the beginning of a compression region.

Method of Characteristics

The sonic lines obtained from one of the interferograms of the flow about the wedge and from one of the flow about the hexagon were used to determine how well the flow field, and particularly the Mach number distributions on the surface, between the sonic line and the main shock wave could be calculated by the method of characteristics. The calculations were made with a minimum amount of given information, which consisted of the location of the sonic line, the location of the surface, and the amount of turning of the flow at a corner. The calculated flow field and surface distribution were then compared with those obtained from the interferogram. The amount of error that could be tolerated in the location of the sonic line without obtaining very inaccurate surface distributions was indicated by these calculations.

Wedge.- For the calculation of the flow about the wedge, the location of the sonic line as given by figure 3(e) was used. Because the size of the bubble of separated flow was unknown and also very small, its existence was not taken into account. The sonic line and oblique shock wave were drawn to meet the surface at the same point, and the flow was assumed to turn through a centered expansion between the sonic line and the shock wave. The surface of the wedge was assumed to be the apparent outer edge of the boundary layer in the interferogram. The lattice-point method of characteristics was used; a characteristic was drawn for each 0.5° turning of the flow; a large scale of 500 times actual size was used in the construction of the initial portion of the network; and second-order effects (the cusps of the characteristics at the sonic line and reflections from the oblique shock wave) were neglected. The resulting network of characteristics, with many of the characteristics that originate near the leading edge omitted because of the small scale of the figure, is shown in figure 6. For comparison, the contours are shown on which the Mach number is 1.356 that were obtained by the method of characteristics and by analysis of the interferogram. The agreement between the results of the two methods is reasonably good. (The disagreement amounts to 4 percent or less in Mach number.) The method of characteristics has, therefore, been shown to be capable of giving the flow field in front of the oblique shock wave reasonably accurately from only the minimum information of the location of the sonic line and the amount of turning.

In this case the method of characteristics also gives the flow along the surface accurately. The Mach number distributions along the surface between the oblique shock wave and the normal shock wave are shown in figure 7. The agreement is excellent; the two distributions agree within one-half of one percent.

Hexagon.- The flow behind the sonic line at the first corner on the hexagon was also calculated by the method of characteristics. The given information for the calculations was the sonic line from figure 5(e) and the two straight lines that form the corner. Because the corner appears to be rounded off by the boundary layer, the corner was represented by an arc of a circle that was tangent at each end to the lines that formed the corner. Over the first half of the circular arc, expansions were started at the surface at intervals of $1/4^{\circ}$ of turning of the surface, and over the other half at intervals of $1/2^{\circ}$. Some of the characteristics are shown in the network of figure 8.

For the purpose of comparing the results of the method of characteristics with the analysis of the interferogram, the contour on which the Mach number was 1.314 was obtained by both methods. The two contours are shown in figure 8 and are seen to be in reasonably close proximity to each other. For the flow along the horizontal surface of the hexagon, behind the first corner, the Mach number distributions given by the two methods are shown by the solid curves of figure 9. The agreement is not good. At 0.6 chord, for example, the method of characteristics gives a Mach number of 1.34, whereas the interferogram gives a Mach number of 1.26. This 6-percent difference in Mach number amounts to a 9-percent difference in pressure. Another calculation was therefore made by the method of characteristics to determine whether the difference in Mach number distribution on the surface shown in figure 9 could be attributed to uncertainty in the location of the sonic line due to errors in the analysis of the interferogram. The systematic errors in the analysis of the interferogram had been estimated to be ±3 percent. The sonic line was therefore thought to lie between the limits that the analysis had given as the contour of Mach number 0.97 and the contour of Mach number 1.03. The 1.03 contour was then assumed to be the sonic line and the calculation by the method of characteristics was repeated for the new sonic line. A revised surface distribution of Mach number was thus obtained and is shown by the dashed curve in figure 9. The surface Mach numbers given by the interferogram were decreased by 0.03 and are also shown in figure 9. The two revised distributions agree very well. Thus, an error in the location of the sonic line amounting to 3 percent in Mach number causes errors in the surface pressure distribution calculated by the method of characteristics that are probably too large to be tolerable. For the method of characteristics to be used for calculating the pressure distribution accurately, the location of the sonic line must apparently be known to within about 1 percent.

In order to calculate the effect of alterations in the contour of an airfoil behind the sonic line (for example, in order to find an optimum contour), the method of characteristics can be used. The location of the sonic line for the original contour can be determined experimentally and the location can be checked and corrected as was done here. Then calculations to give pressure distributions when alterations are made in the contour (behind the sonic line) can then be made by the method of characteristics without the need for additional tests on the altered contours.

Drag Coefficient of Wedge of 14.5° Semiangle

The pressure drag coefficient of the wedge forepart of the hexagon was obtained from the interferograms. First, the contours of figure 5 were used for plotting in figure 10 the Mach number distributions between the leading edge and the first corner. The Mach number distributions are converted into pressure distributions in figure 11.

The pressure drag coefficients for the wedge forepart of the hexagon (for zero angle of attack of the chord line and based on the assumption of free-stream pressure on the base of the wedge) were then obtained by integration of the pressure distributions. (The drag coefficients could not be accurately obtained at the three lower Mach numbers, however, partly because the sensitivity of the interferometer is not so great at the lower Mach numbers as it is at the higher ones but mostly because the drag coefficient is obtained as the small difference between two large quantities at the lower Mach numbers but as the difference between a large and a small quantity at the higher Mach numbers.) The drag coefficients at the three higher Mach numbers are expressed according to the transonic similarity laws (for example, ref. 4) and values of the parameter $\frac{\gamma + 1}{\tau^{5/3}} C_D$ are plotted against $\frac{M^2 - 1}{\left[(\gamma + 1)\tau\right]^{2/3}}$ in figure 12. (The quantity τ is the thickness ratio of the symmetrical wedge that would be formed by eliminating the middle portion of the hexagon and joining the wedge forepart and the wedge afterpart.) The other data of figure 12 were taken from figure 13 of reference 2 and show the variation of drag coefficient of three wedges of smaller angle (4.5°, 7.5° and 10° semiangle) than the wedge tested in the present experiments (14.5° semiangle). The present results are seen to be consistent with those for wedges of smaller angle.

Conditions at Bases of Shock Waves

In reference 3 boundary conditions at the bases of shock waves that interacted with a turbulent boundary layer on a circular-arc section were investigated. As a continuation of that work, boundary conditions on the shock waves on the wedge have been determined. Each of figures 3(c), 3(d), and 3(e) shows two shock waves near the leading edge of the wedge, the first of which interacts with a laminar boundary layer and the second with a turbulent boundary layer. Thus, comparisons can be made between the conditions at the interaction of a shock wave with a turbulent boundary layer on the circular-arc section and on the wedge and also between the conditions at the interaction of the shock wave with both a laminar boundary layer and a turbulent boundary layer on the wedge. The conditions at the bases of the shock waves on the wedge are shown in table I. The densities ρ_1 and ρ_2 were taken from the interferograms. The Mach number M_1 was determined from ρ_1 and M_o. The observed shock-wave angle ϵ was measured on the interferogram. The calculated shock-wave angle ϵ was calculated from the measured values of ρ_2/ρ_1 and M_1. The pressure ratio was calculated from the density ratio, and $\Delta p/q_1$ was calculated from the equation.

$$\frac{\Delta p}{q_1} = \frac{\frac{p_2}{p_1} - 1}{\frac{\gamma}{2} M_1{}^2}$$

Within the limits of the accuracy of the tests, both p_2/p_1 and $\Delta p/q_1$ are constant for each type of boundary layer over the range of variables covered by the tests. The range of variables is, however, small.

In the investigation reported in reference 3 of the interaction of a shock wave with a turbulent boundary layer on a circular-arc airfoil, the value of p_2/p_1 was found to be essentially the same, 1.4, as the value obtained in the present case for the normal shock wave. The value of $\Delta p/q_1$ for the circular-arc section was approximately 0.3 and, in the present case, is approximately 0.4. The equilibrium condition at the base of a shock wave undoubtedly depends on the Reynolds number of the boundary layer, but the range covered by the tests is too small to show definitely the effect of Reynolds number.

The intensity of the shock wave that is in equilibrium with the laminar boundary layer is seen to be much less than that of the shock wave that is in equilibrium with the turbulent boundary layer. The value of $\Delta p/q_1$ when the boundary layer is laminar is only about 5 percent as large as when the boundary layer is turbulent.

CONCLUDING REMARKS

The two types of flow configuration at the leading edge of a wedge at an angle of attack greater than the semiangle of the wedge were observed with an interferometer.

The supersonic region at the corner on a hexagonal profile was observed and Mach number contours in the flow field were obtained. These data may be of value in future efforts to calculate theoretically the flow fields. The pressure drag coefficient of the wedge forepart of the hexagon of 14.5° semiangle, which was measured at Mach numbers from 0.768 to 0.854, was found to be consistent with those of wedges of smaller angles when plotted in terms of the transonic similarity parameters.

It was demonstrated that the flow fields between the sonic line and the oblique shock wave on the hexagon and the wedge could be calculated rather accurately by the method of characteristics if the locus of the sonic line and the geometry of the surface were given. It was also shown that the location of the sonic line must be known to within about 1 percent (in Mach number) for the calculation to give the pressure distribution on the surface behind the sonic line accurately.

The conditions at the bases of shock waves that interacted with boundary layers on a wedge were determined. The ratio of the pressure difference across the shock wave to the dynamic pressure ahead of the shock wave $\Delta p/q_1$ was found to have a value of about 0.4 when the boundary layer was turbulent and about 0.02 when the boundary layer was laminar.

Langley Aeronautical Laboratory,
National Advisory Committee for Aeronautics,
Langley Field, Va., September 18, 1952

REFERENCES

1. Lindsey, W. F., Daley, Bernard N., and Humphreys, Milton D.: The Flow and Force Characteristics of Supersonic Airfoils at High Subsonic Speeds. NACA TN 1211, 1947.

2. Bryson, Arthur Earl, Jr.: An Experimental Investigation of Transonic Flow Past Two-Dimensional Wedge and Circular-Arc Sections Using a Mach-Zehnder Interferometer. NACA TN 2560, 1951.

3. Wood, George P., and Gooderum, Paul B.: Investigation With an Interferometer of the Flow Around a Circular-Arc Airfoil at Mach Numbers Between 0.6 and 0.9. NACA TN 2801, 1952.

4. Von Kármán, Th.: The Similarity Law of Transonic Flow. Jour. Math. and Phys., vol. XXVI, no. 3, Oct. 1947, pp. 182-190.

TABLE I.- CONDITIONS AT BASES OF SHOCK WAVES ON WEDGES

Figure	M_o	$\frac{\rho_2}{\rho_1}$	M_1	ϵ(observed), deg	ϵ(calculated), deg	$\frac{p_2}{p_1}$	$\frac{\Delta p}{q_1}$
Laminar boundary layer (Oblique shock wave)							
3(c)	0.812	1.028	1.60	--	39.5	1.045	0.025
3(d)	.854	1.026	1.55	--	41	1.036	.021
3(e)	.894	1.024	1.57	--	40	1.034	.020
Turbulent boundary layer ("Normal" shock wave)							
3(c)	0.812	1.285	1.21	74	75	1.43	0.42
3(d)	.854	1.26	1.20	78	74	1.38	.38
3(e)	.894	1.28	1.22	90	73	1.42	.40

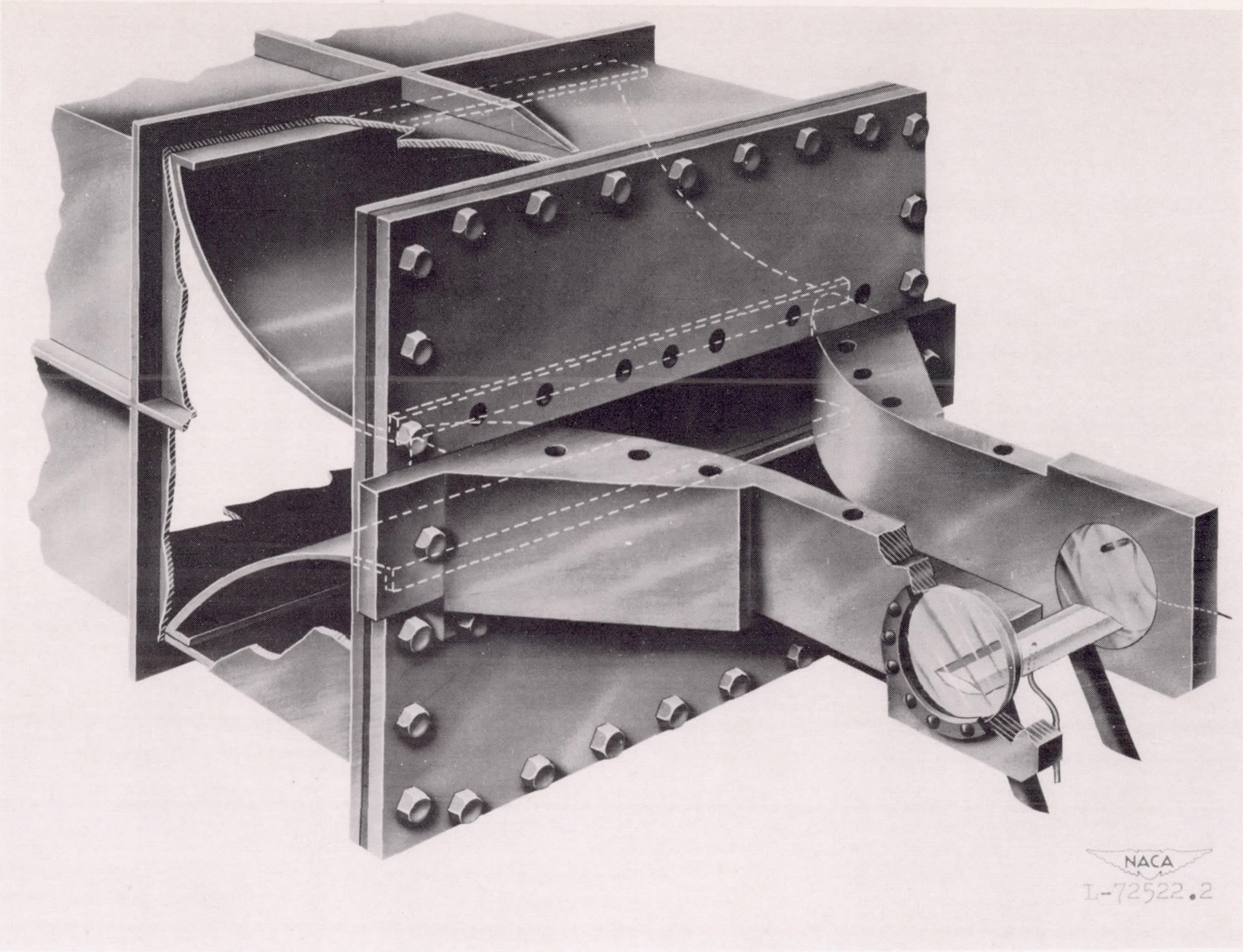

Figure 1.- Nozzle and test section showing model installation.

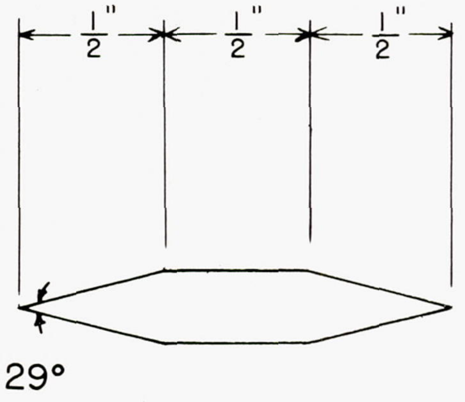

(a) Hexagon.

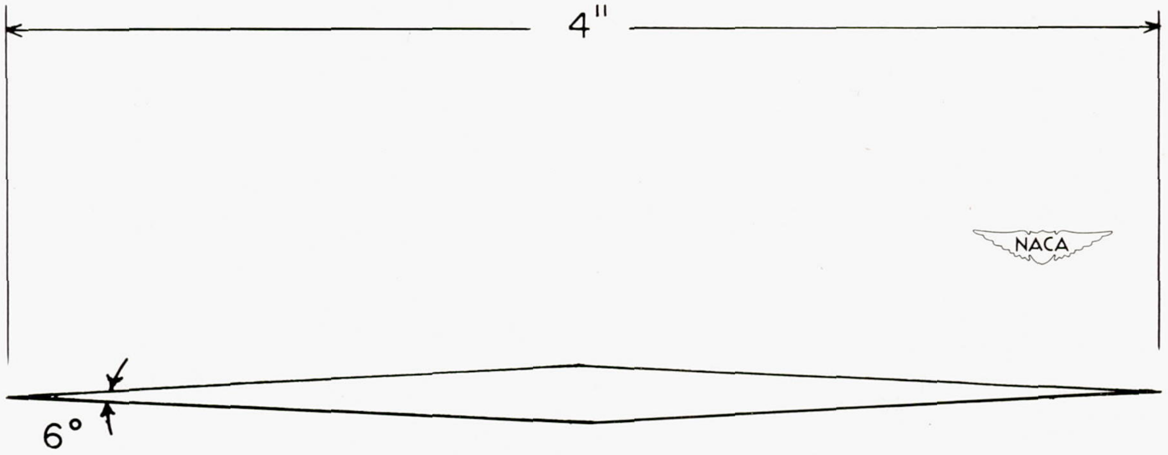

(b) Symmetrical wedge.

Figure 2.- Models.

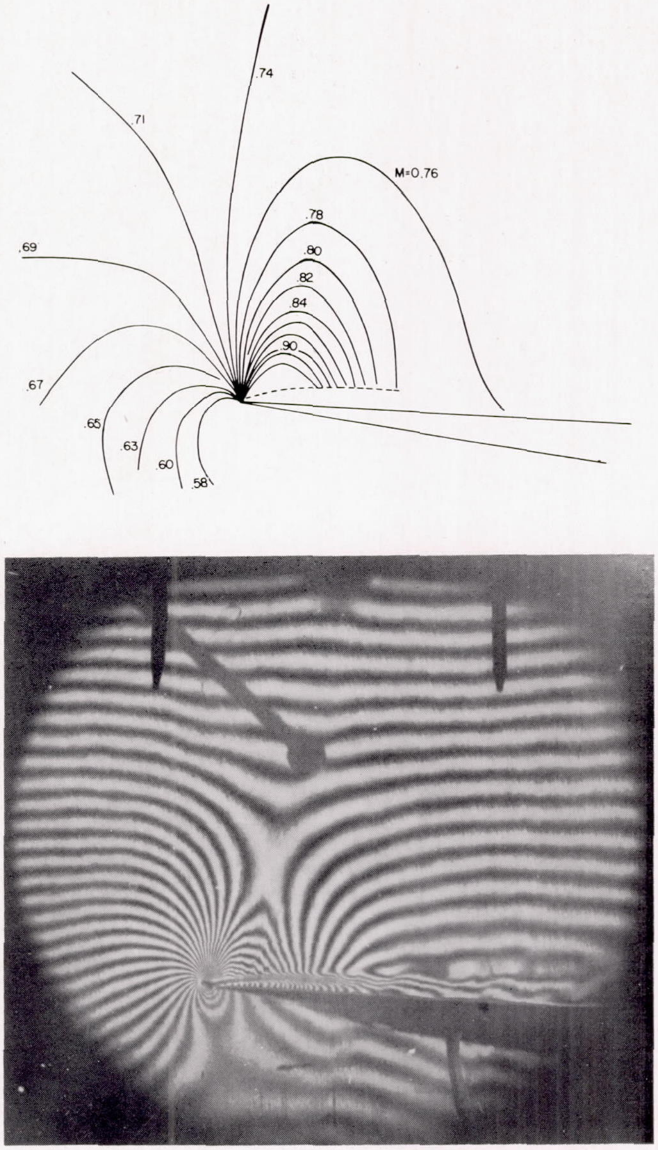

(a) $M_o = 0.721$.

L-76188

Figure 3.- Interferograms and Mach number distributions of the flow about the leading edge of a wedge. $\alpha = 5.5^\circ$.

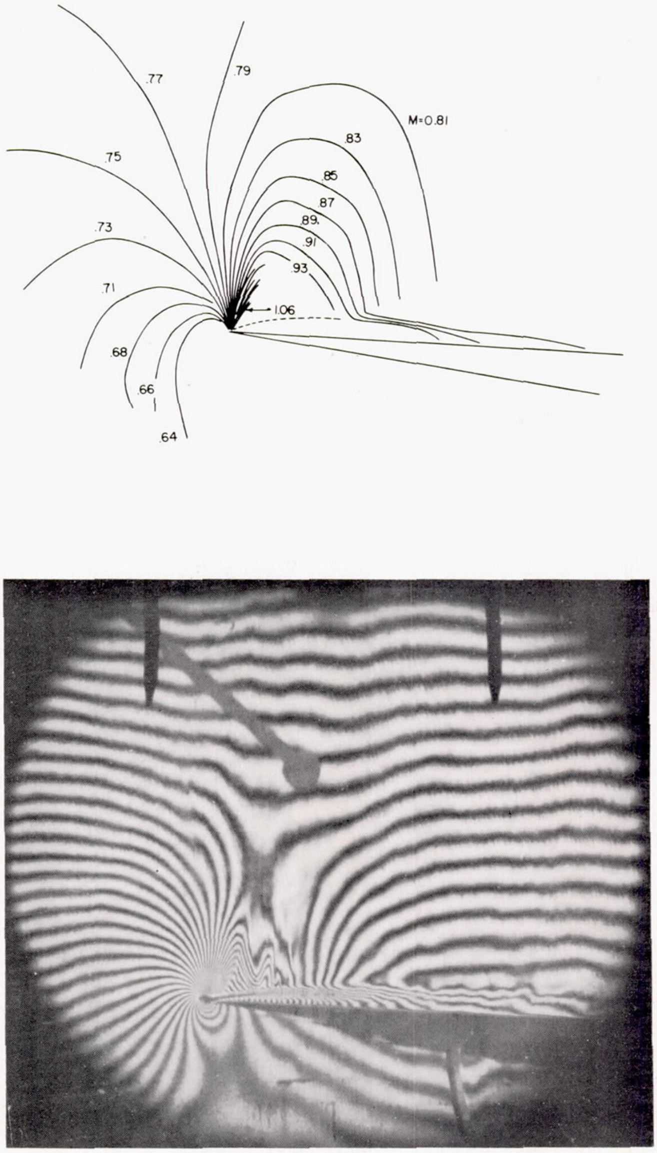

(b) $M_o = 0.765$.

L-76189

Figure 3.- Continued.

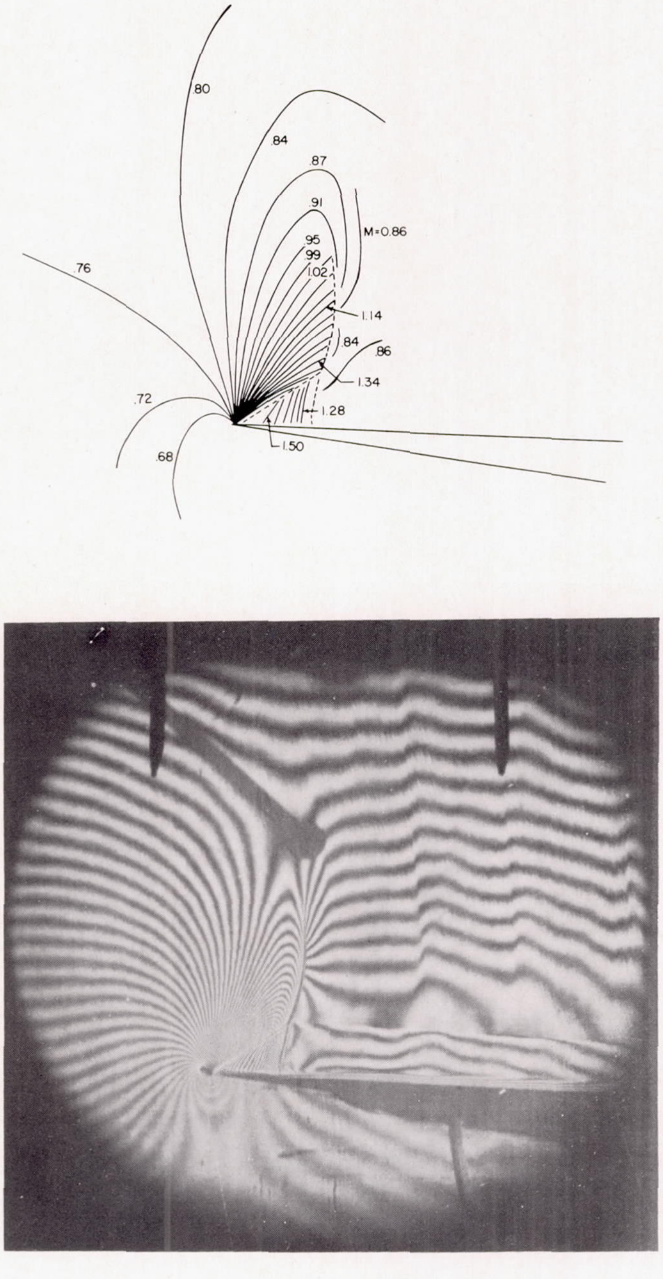

(c) M_o = 0.812.

L-76190

Figure 3.- Continued.

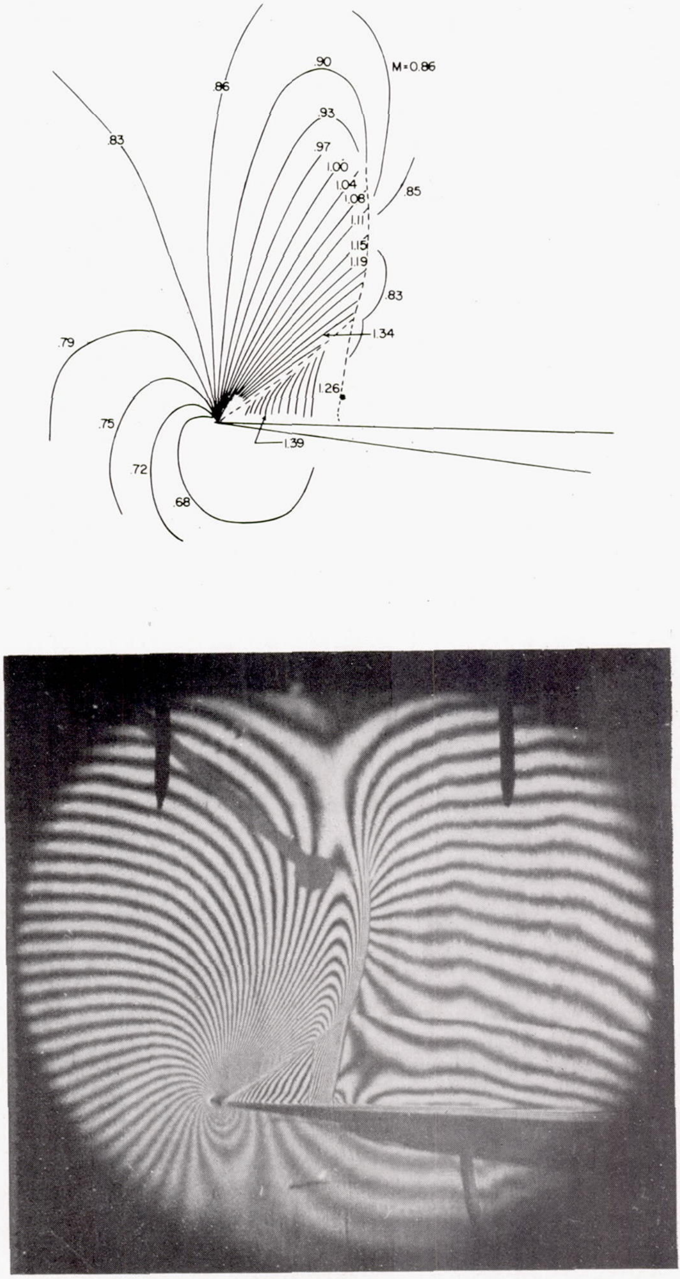

(d) $M_o = 0.854$.

NACA
L-76191

Figure 3.- Continued.

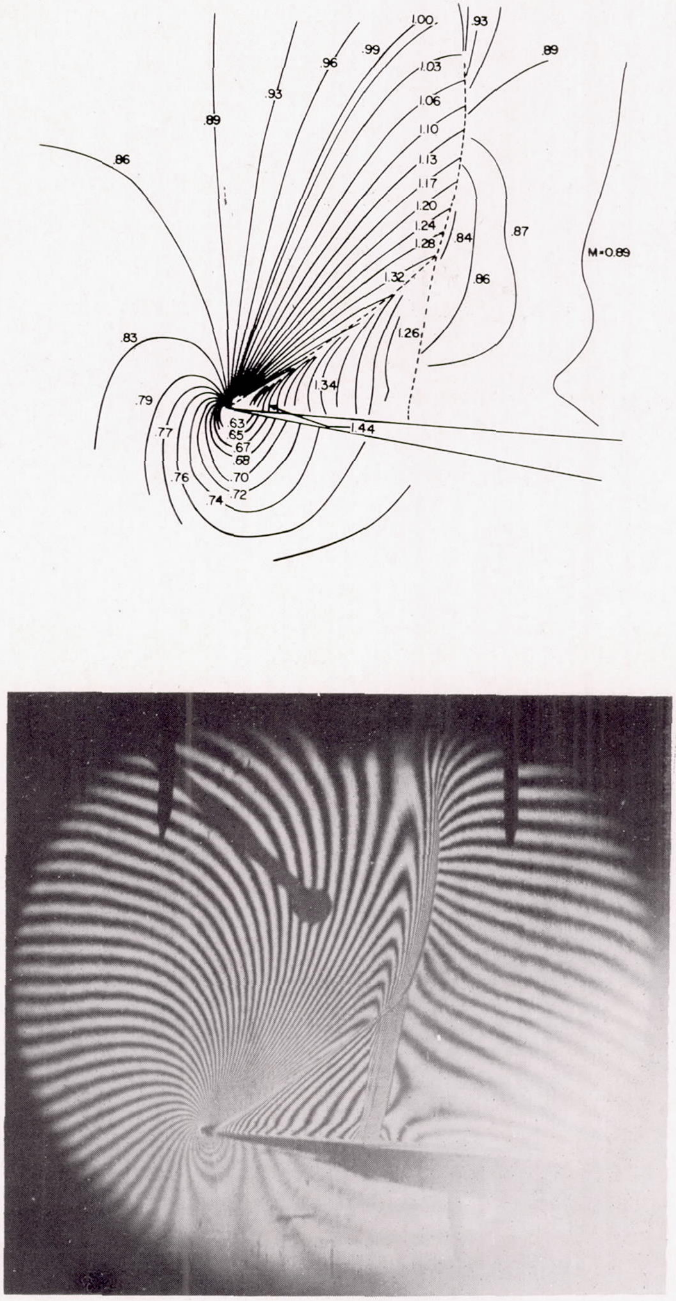

(e) $M_o = 0.894$.

L-76192

Figure 3.- Concluded.

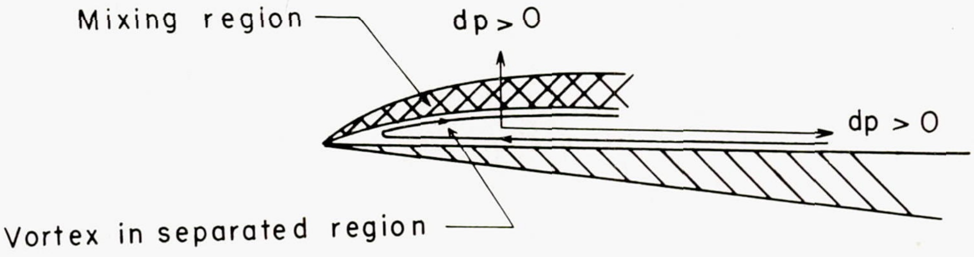

(a) Large separated region.

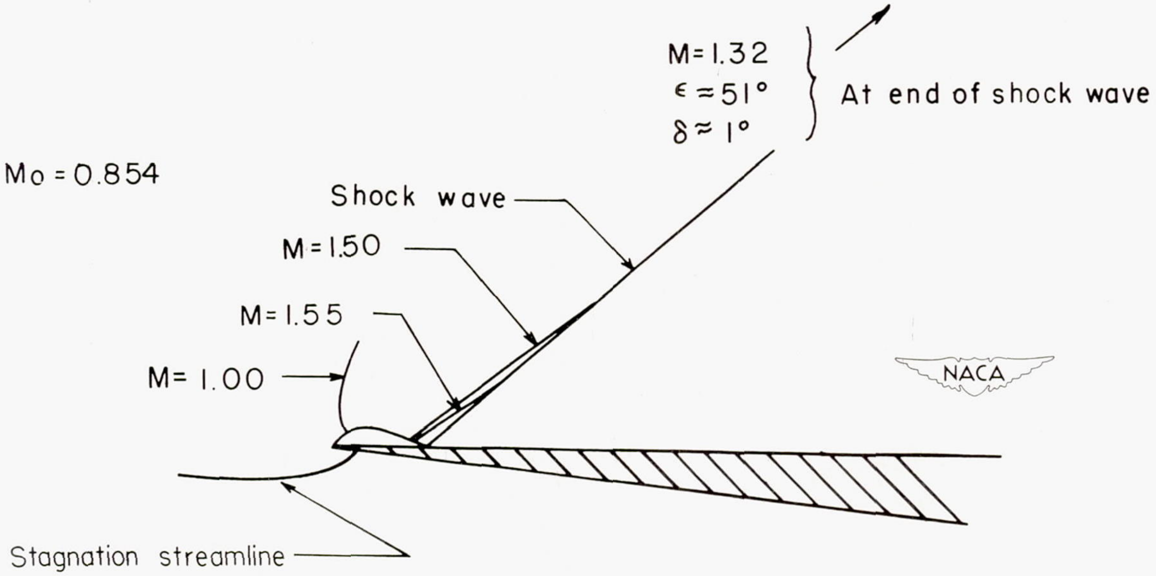

(b) Very small separated region.

Figure 4.- Flow configurations near leading edge.

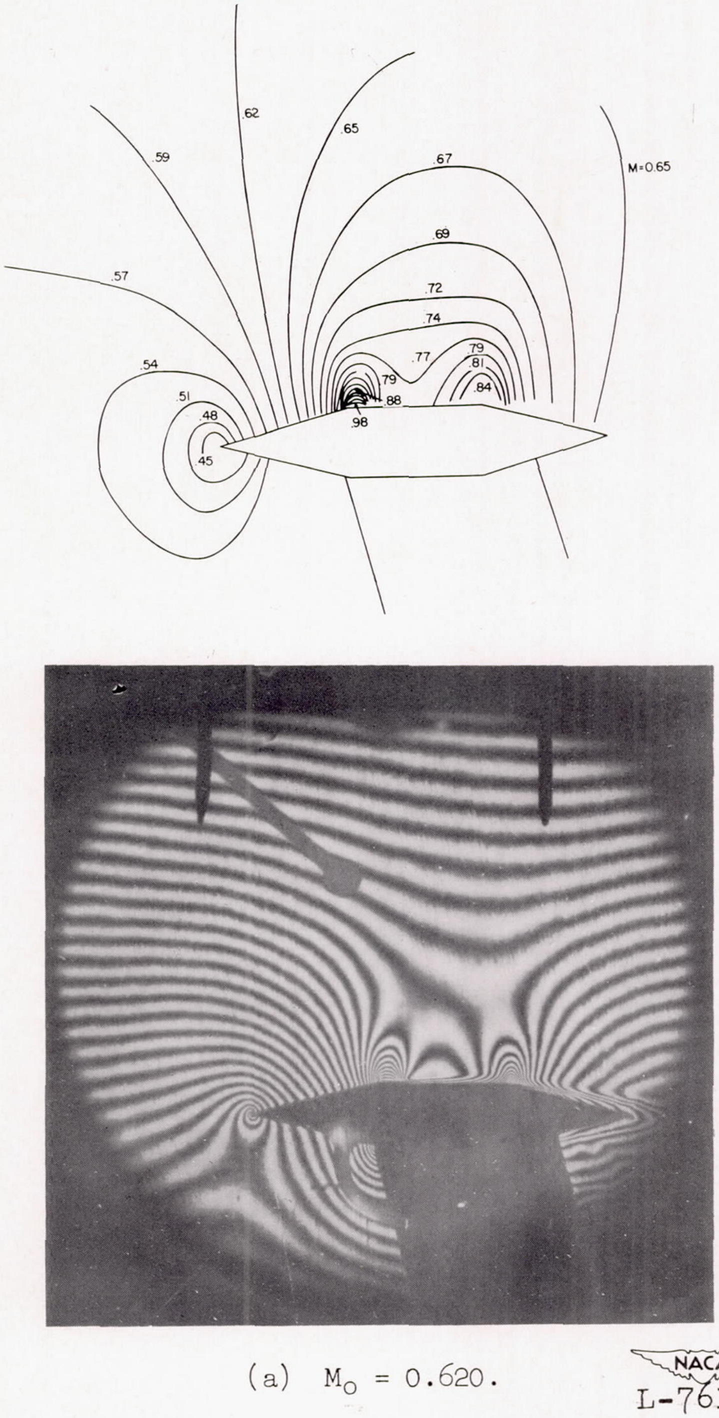

(a) $M_o = 0.620$.

L-76193

Figure 5.- Interferograms and Mach number distributions of the flow about a hexagon. Wedge semiangle, 14.5°; $\alpha = 0^{\circ}$.

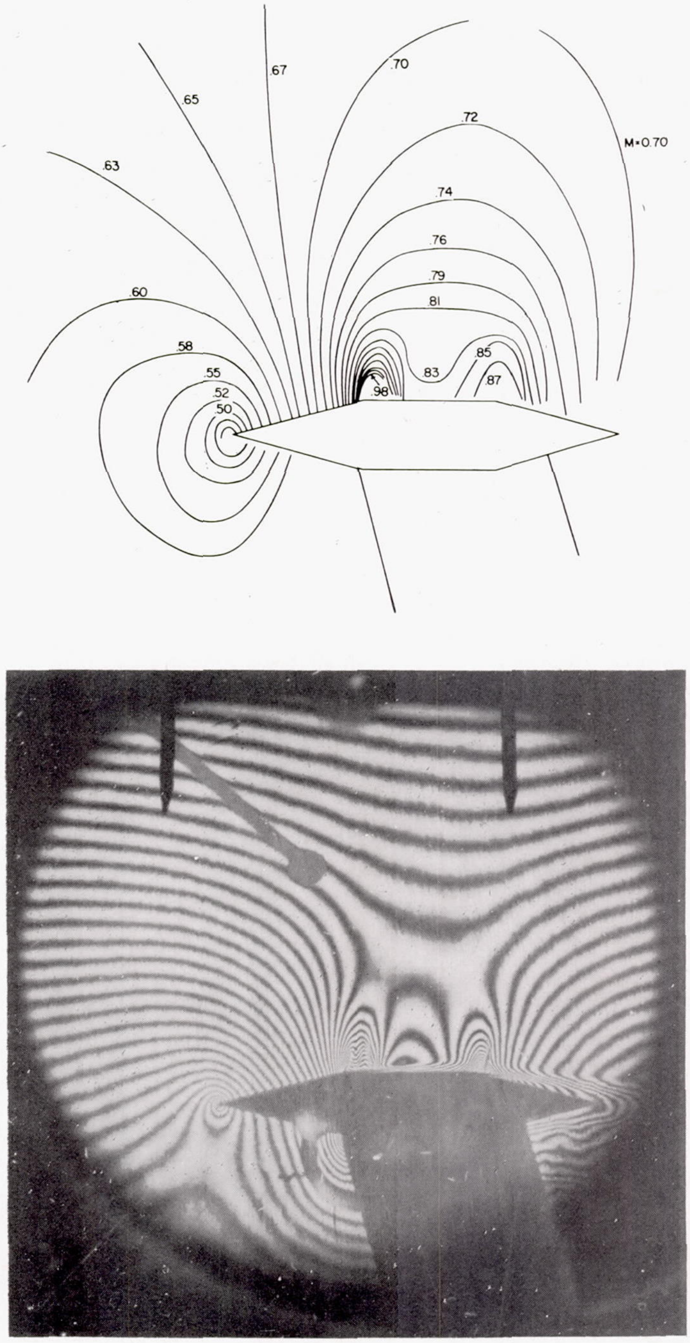

(b) $M_o = 0.667$.

L-76194

Figure 5.- Continued.

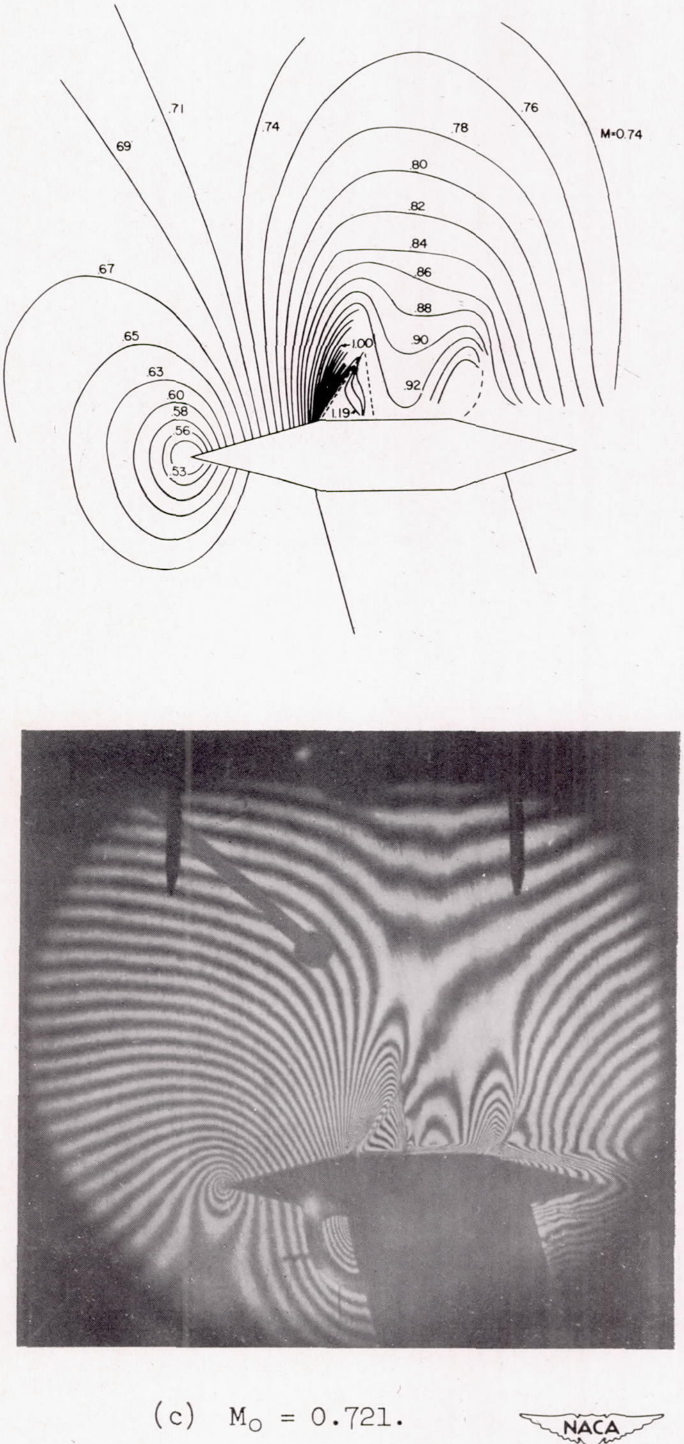

(c) $M_o = 0.721$.

L-76195

Figure 5.- Continued.

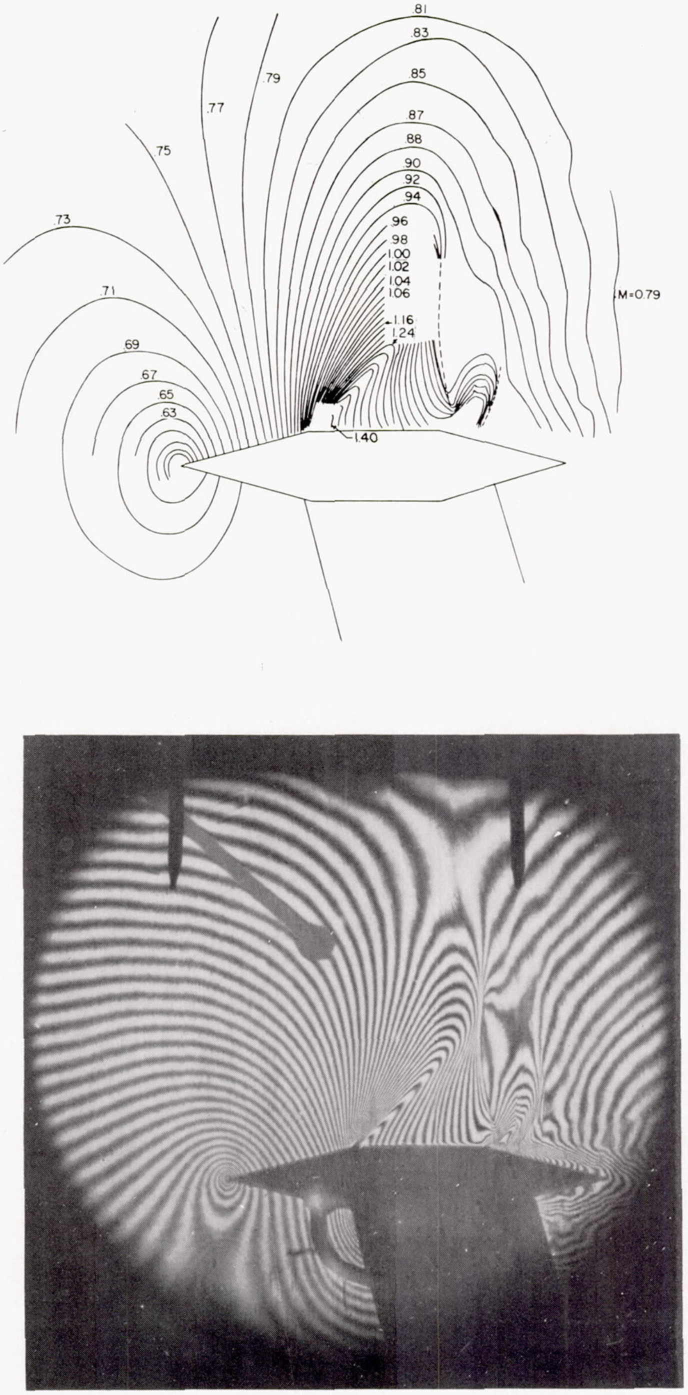

(d) $M_o = 0.768$.

L-76196

Figure 5.- Continued.

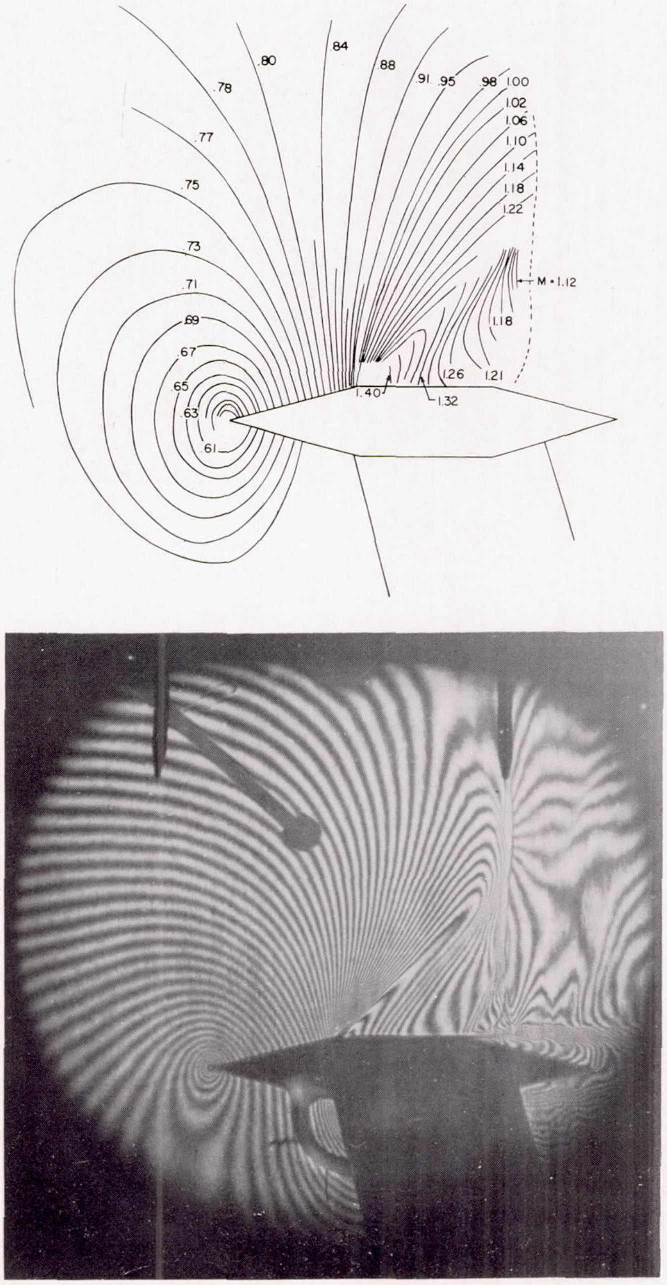

(e) $M_0 = 0.819$.

L-76197

Figure 5.- Continued.

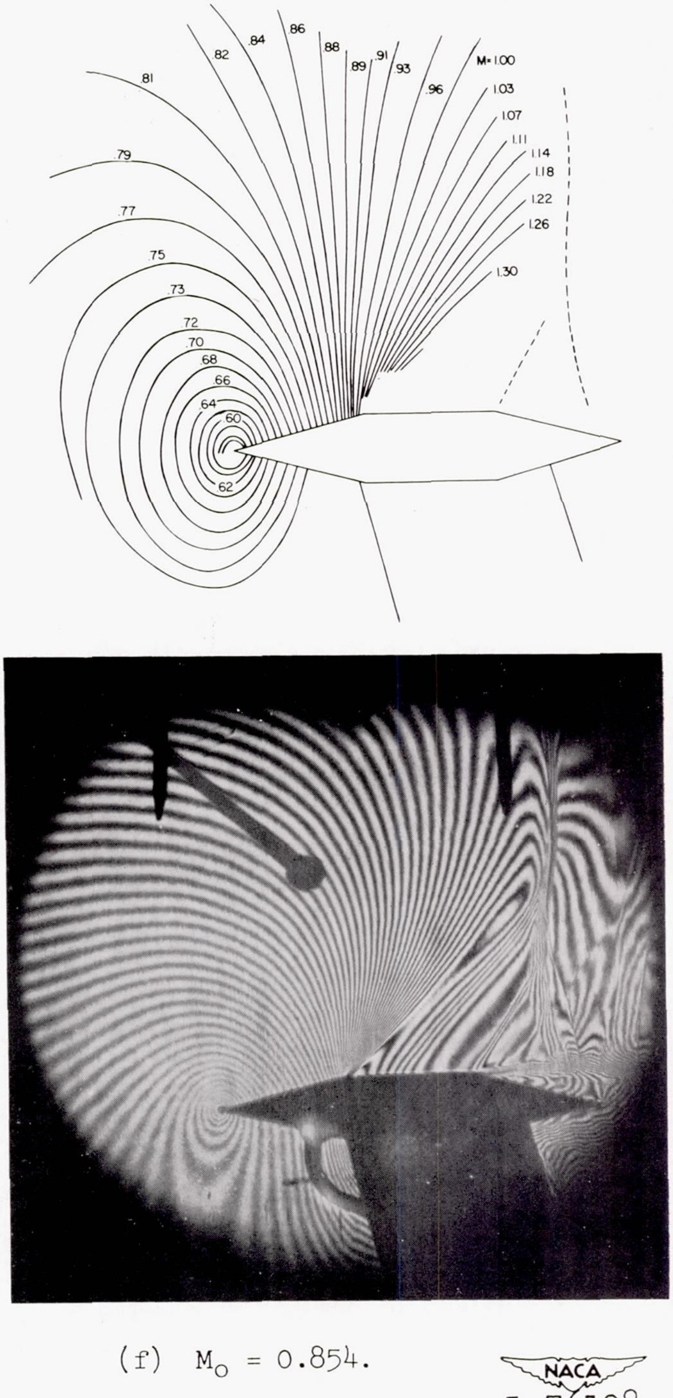

(f) $M_o = 0.854$.

NACA
L-76198

Figure 5.- Continued.

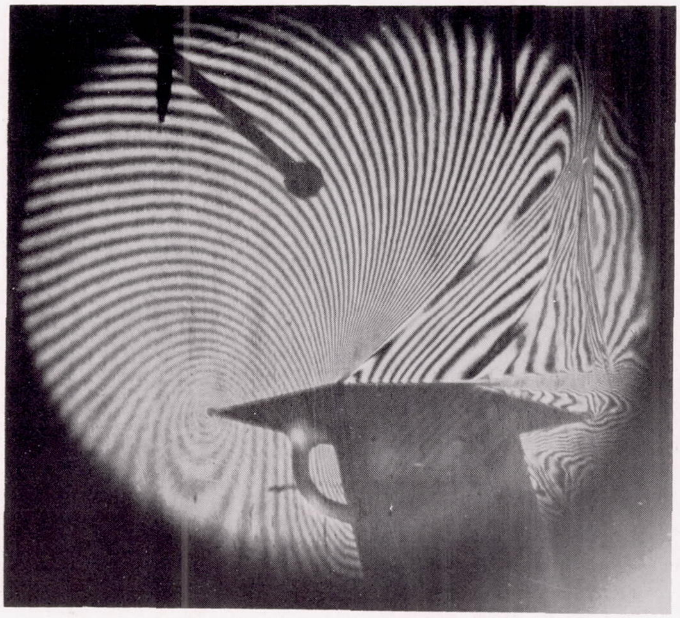

(g) $M_o = 0.889$.

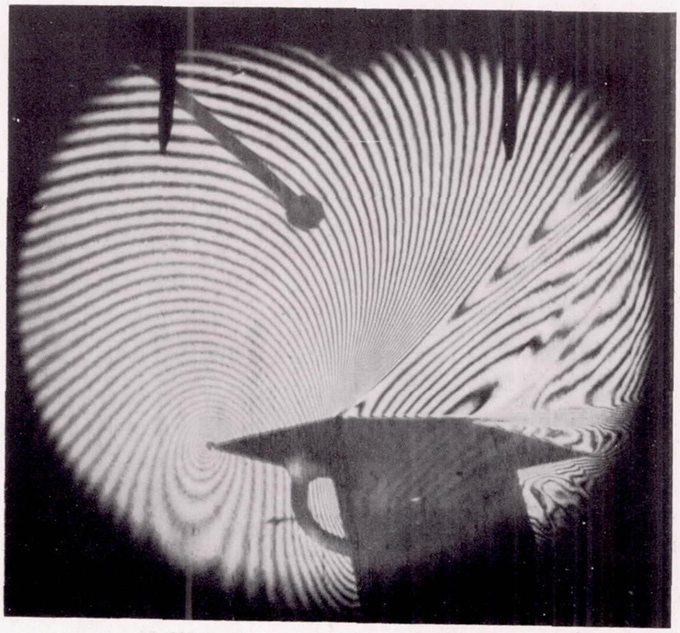

(h) $M_o = 0.933$.

L-76199

Figure 5.- Concluded.

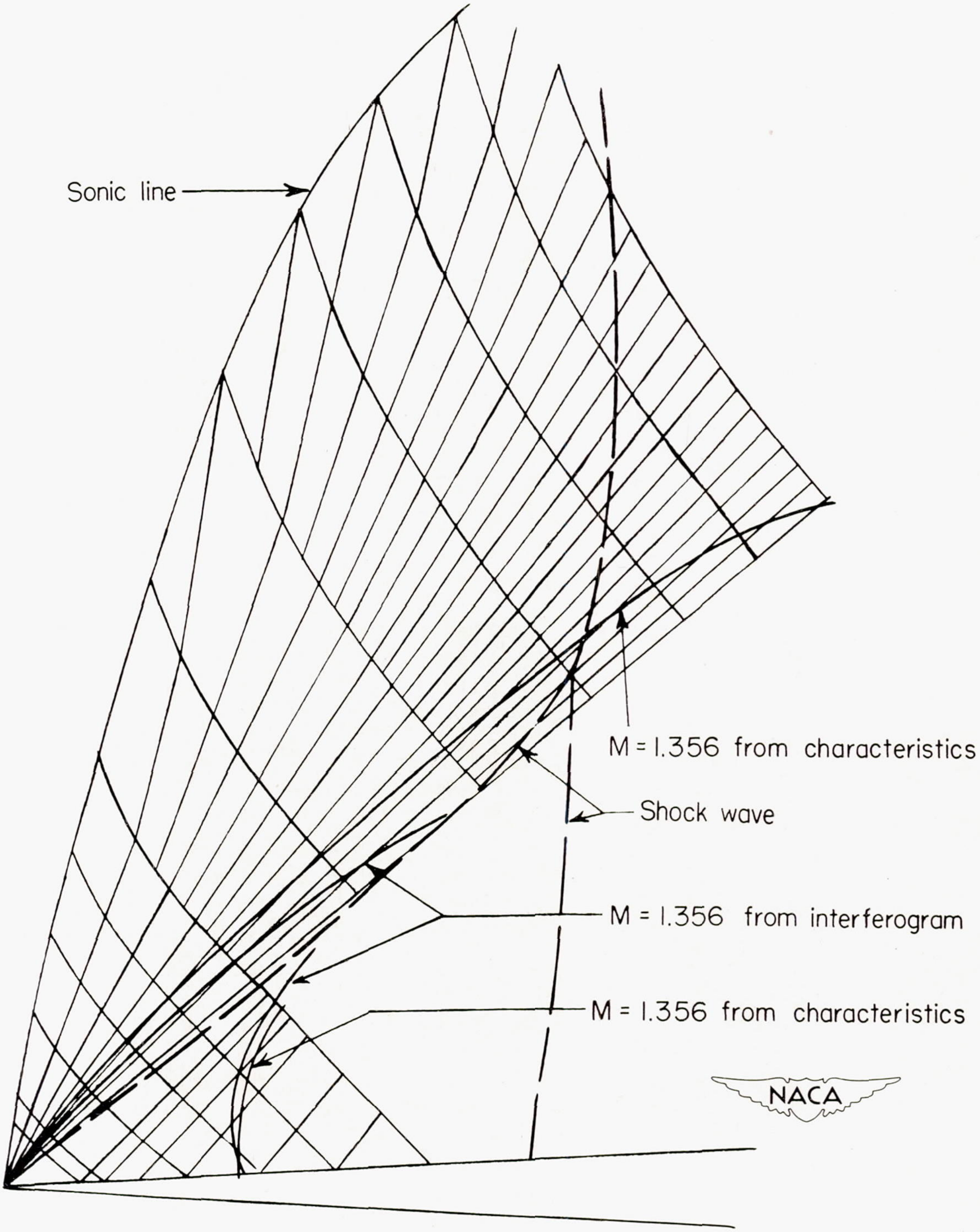
Sonic line
M = 1.356 from characteristics
Shock wave
M = 1.356 from interferogram
M = 1.356 from characteristics

Figure 6.- Characteristic network for flow about leading edge of wedge. $\alpha = 5.5^{\circ}$; $M_o = 0.894$.

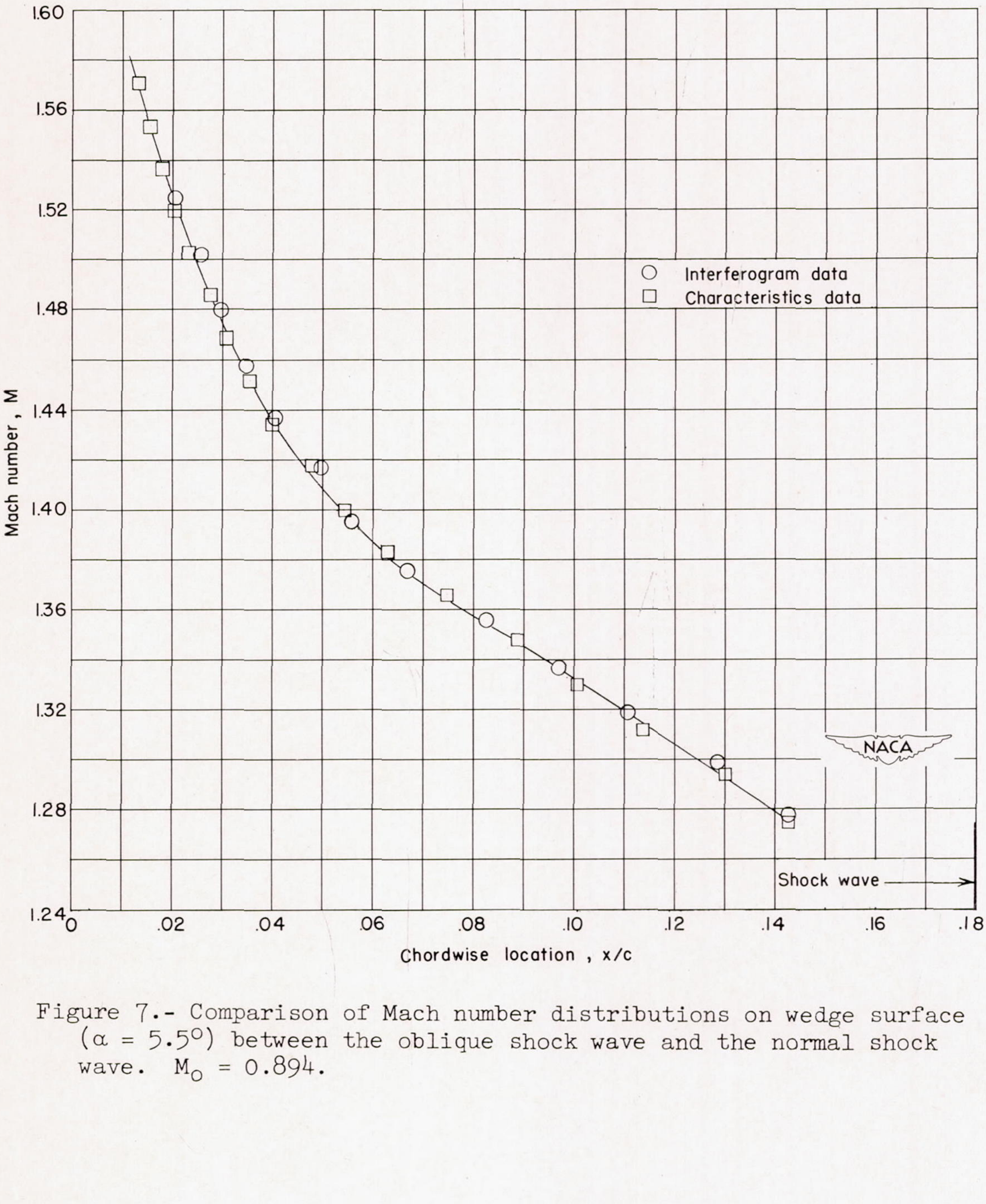

Figure 7.- Comparison of Mach number distributions on wedge surface ($\alpha = 5.5^{\circ}$) between the oblique shock wave and the normal shock wave. $M_o = 0.894$.

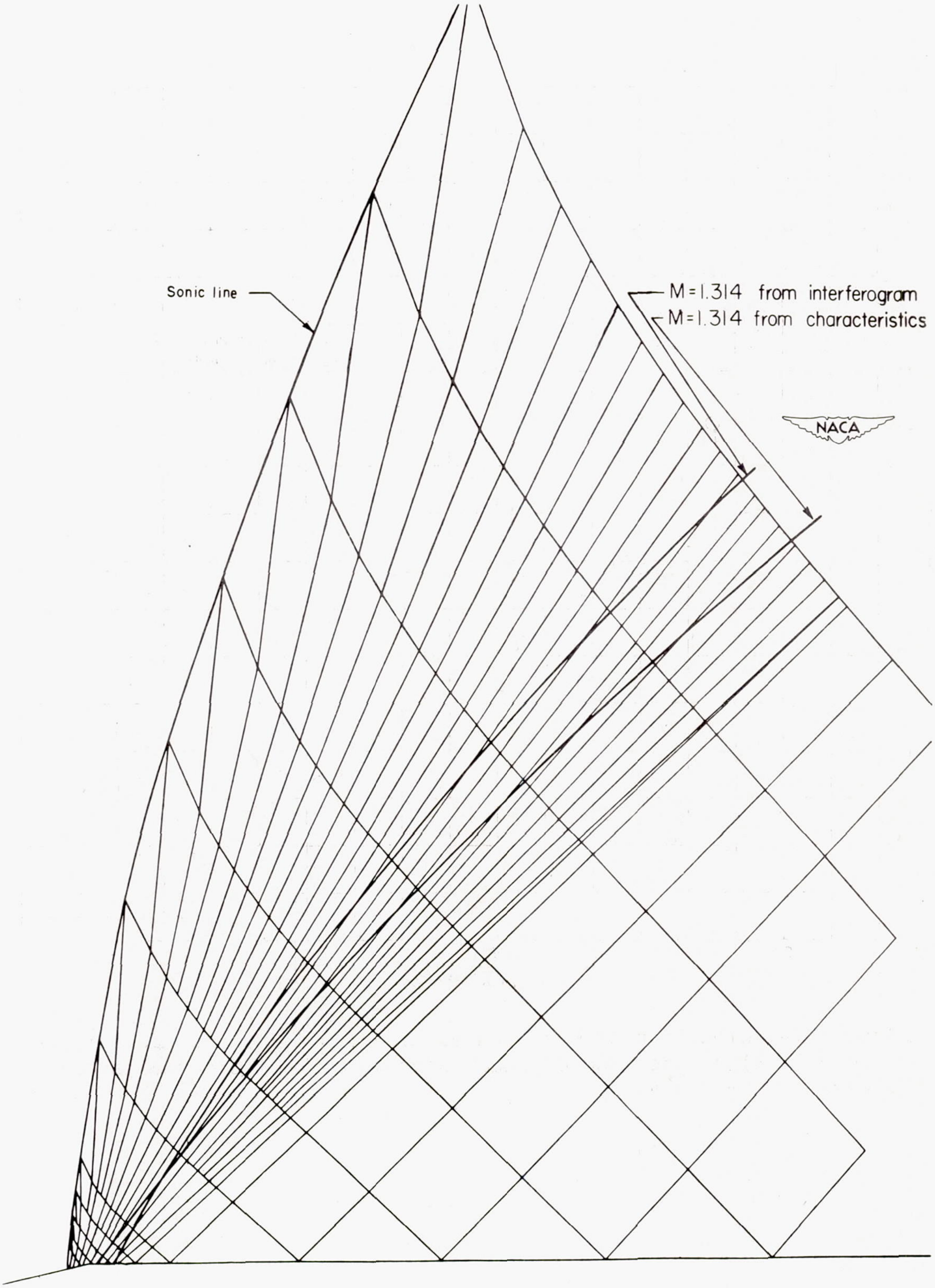

Figure 8.- Characteristic network for flow around hexagon. $M_o = 0.819$.

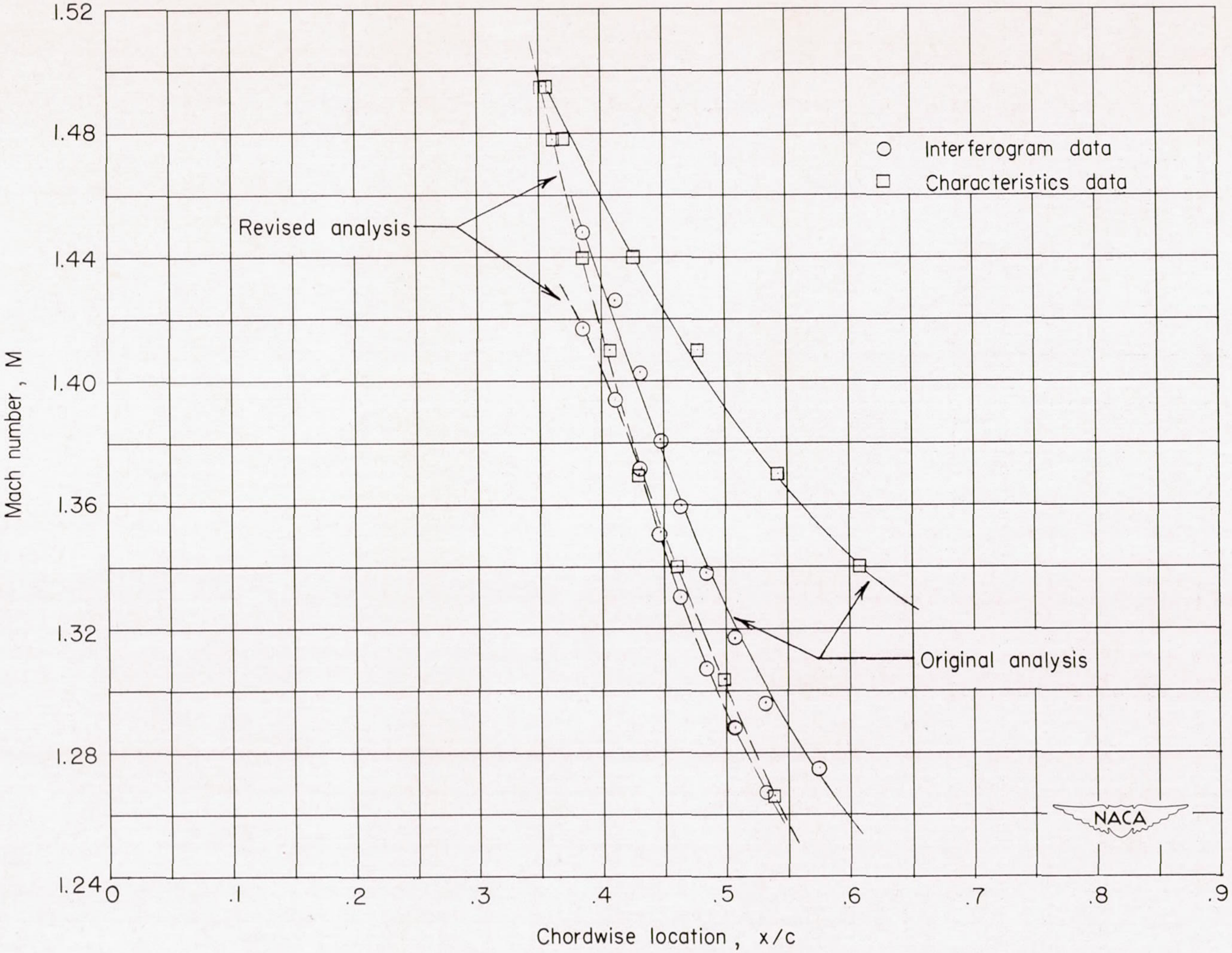

Figure 9.- Comparison of Mach number distributions on horizontal surface of hexagon behind corner. $M_o = 0.819$.

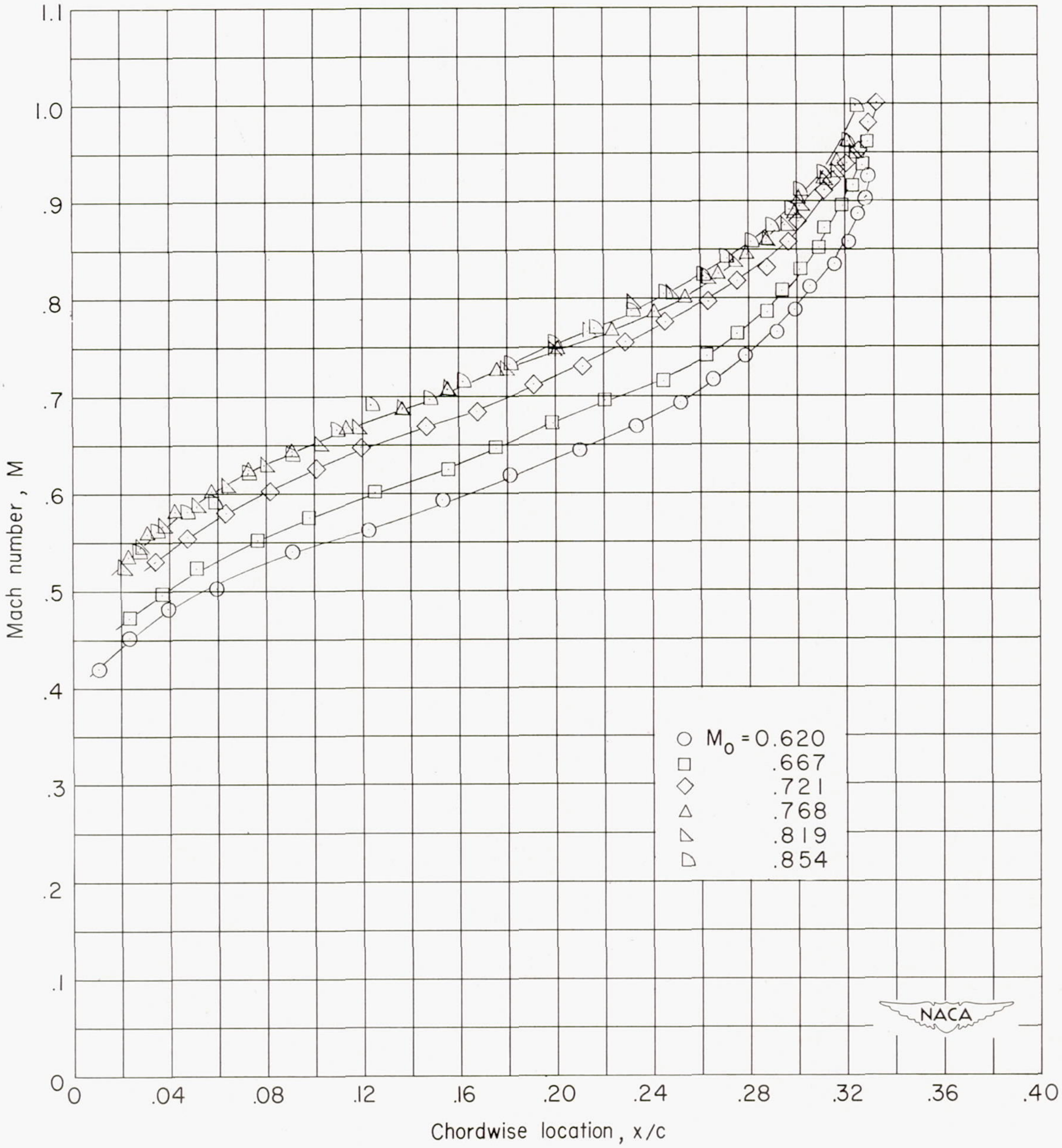

Figure 10.- Mach number distributions on surface of hexagon between leading edge and first corner. (14.5° semiangle wedge.)

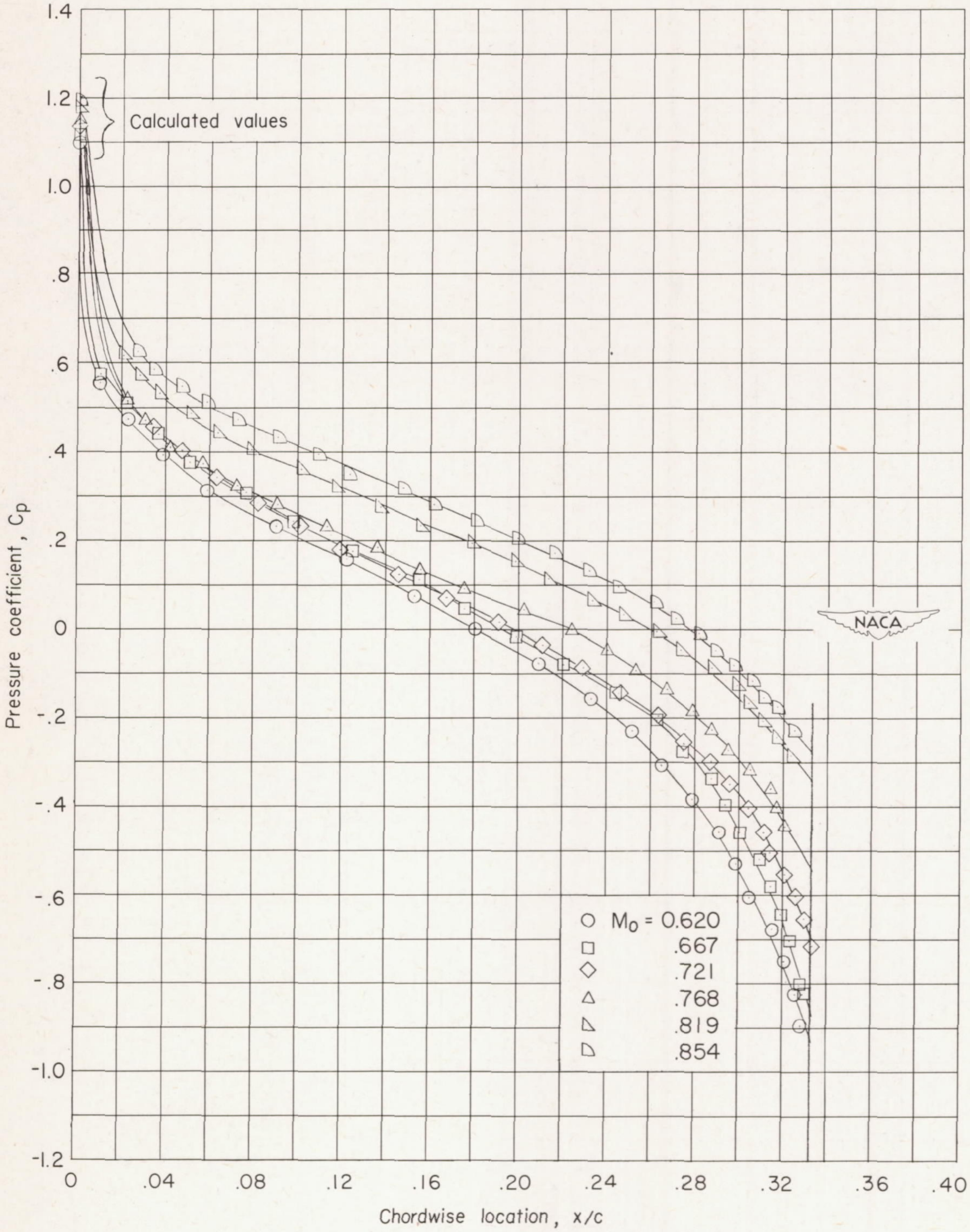

Figure 11.- Pressure distributions on surface of hexagon between leading edge and first corner. (14.5° semiangle wedge.)

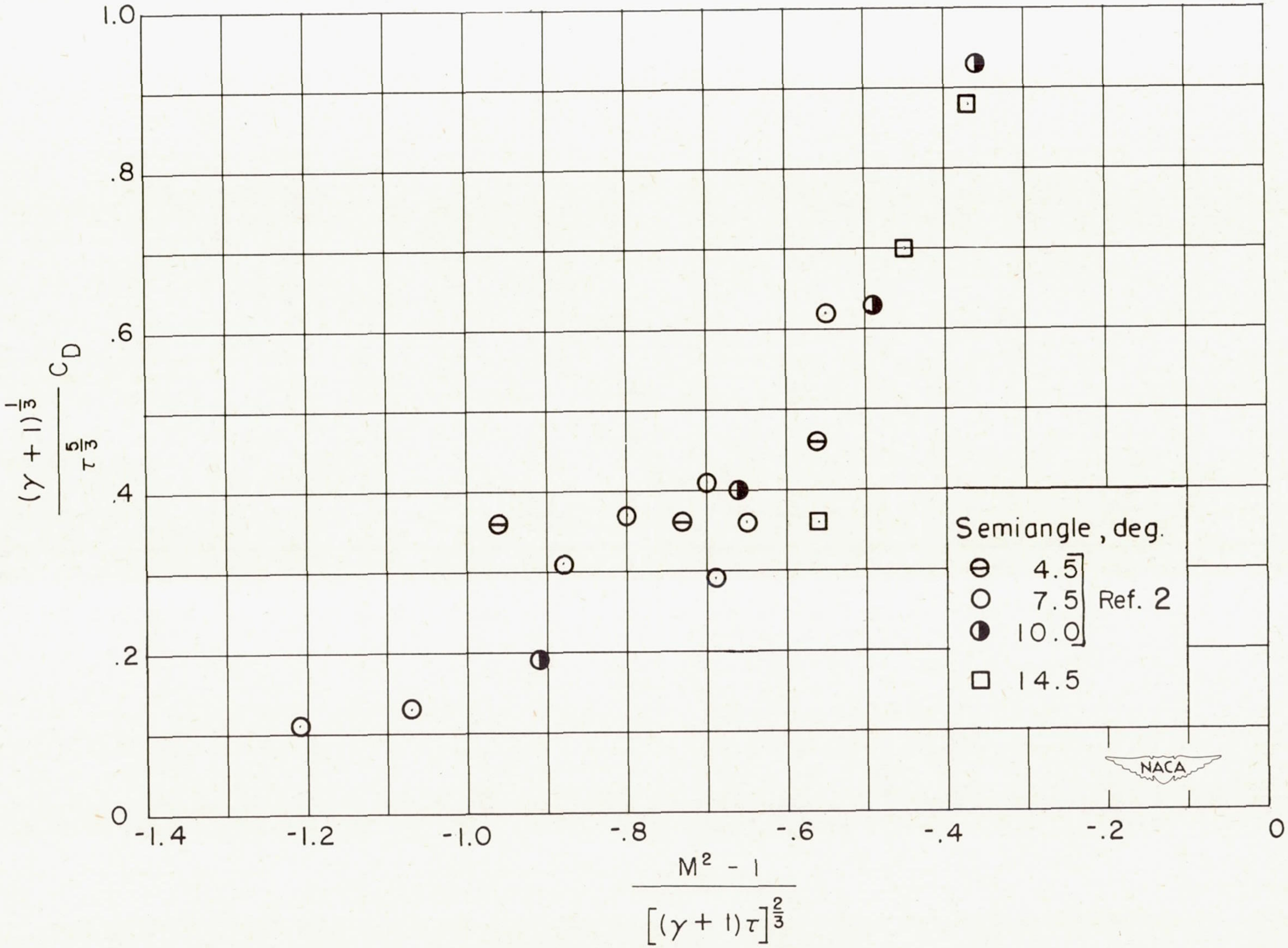

Figure 12.- Function of C_D against function of M, with variables expressed according to transonic similarity law.

NACA-Langley - 11-14-52 - 1000